Distinct effects of contour smoothness and observer bias on visual persistence

Zhiheng Zhou

Department of Psychology, University of Nevada, Reno, NV, USA

Lars Strother

Department of Psychology, University of Nevada, Reno, NV, USA

Stable object perception relies on persistent yet temporary neural representations under constantly fluctuating stimulus conditions. The mechanisms by which such representations are formed and maintained are not fully understood but presumably involve interplay between early and higher tier visual cortical mechanisms. Some neurophysiological models of feature binding in early visual cortex predict persistent contour perception under certain stimulus conditions. Here we show that the duration of contour persistence reflects the persistent operation of visual mechanisms sensitive to contour smoothness, which also influences contour visibility more generally under highly camouflaging stimulus conditions. We distinguish the effect of contour smoothness on contour persistence from observer bias, which also contributes to the surprisingly long duration of contour persistence. We conclude that the strong modulatory effects of contour smoothness on persistence are due to the sustained reverberation of local and global contour-binding mechanisms in visual cortex, which form an important basis of perceptual continuity and stable object perception.

Introduction

Contours are powerful indicators of object shape and surface boundaries. Visual sensitivity to the physical properties of contours is consistent with the statistical properties of contours in natural images (Geisler & Perry, 2009; Geisler, Perry, Super, & Gallogly, 2001), and this is often reflected in neurally plausible models of contour integration. For example, the *association-field* model of contour integration binds discrete edge information into perceptually continuous contours through mutual facilitation between visual cortical neurons with similarly oriented classical receptive fields (Field, Hayes, & Hess, 1993). The existence of an association-field and other qualitatively similar contour-integration mechanisms is consistent with patterns of long-range horizontal connections in visual cortex (Sigman, Cecchi, Gilbert, & Magnasco, 2001), as well as an abundance of corroborative psychophysical data. Here we are interested in the possibility that an association-field or similar neural mechanism supports the *persistence* of contour integration, and thus promotes perceptual continuity in both space and time.

Stable perception relies on the capacity of neural circuits to temporarily maintain perceptual representations under constantly changing sensory input. The neural basis of this ability is not fully understood, but it may be partly due to intrinsic memory properties of early visual cortical mechanisms. For example, O'Herron and von der Heydt (2009, 2011) reported persistent figure–ground border-ownership signals in single neurons in visual cortex, which they interpreted as the basis for stable figure–ground segmentation under fluctuating stimulus conditions. The existence of this type of persistent neural activity in visual cortex may be indicative of positive feedback loops within visual cortex (Grossberg, 2015). In the context of contour perception, some have proposed that excitatory feedback circuits bind contour features and exhibit persistence (Francis, 1996; Francis, Grossberg, & Mingolla, 1994). If so, this would imply that persistent contour binding plays a foundational role in stable object perception, a prediction we test here with respect to smoothness sensitivity and the association-field mechanism of contour integration.

Positive-feedback models of contour processing in visual cortex predict that persistent contour binding should occur in the absence of an inhibitory reset signal, such as stimulus offset (Francis, 1999). Perceptual effects consistent with these predictions are evident in a demonstration (https://sites.google.com/site/

Citation: Zhou, Z., & Strother, L. (2017). Distinct effects of contour smoothness and observer bias on visual persistence. *Journal of Vision*, *17*(2):8, 1–12, doi:10.1167/17.2.8.

doi: 10.1167/17.2.8 Received July 25, 2016; published February 28, 2017 ISSN 1534-7362

visualformpersists/) adapted from Regan (1986). In the demonstration, a contour-defined bird becomes visible by virtue of structure from motion, and critically, it persists perceptually even after it stops moving (left demo), but only when the contour segments remain embedded in the camouflaging background (right demo). The duration of this type of *contour persistence* is typically 1–3 s, and contour visibility ends instantaneously when contour elements are physically removed (Ferber, Humphrey, & Vilis, 2003, 2005; Large, Aldcroft, & Vilis, 2005; Strother et al., 2011; Strother, Lavell, & Vilis, 2012), consistent with offset-initiated reset and the prevention of contour "hallucination" in the absence of supporting visual input (Li, 1998). The duration of contour persistence is considerably longer than the neural persistence reported by O'Herron and von der Heydt (2009, 2011) for figure–ground border-ownership signals in visual cortex (0–1.3 s), and it is also longer than any other type of shape-related visual persistence we are aware of (e.g., Bruchmann, Thaler, & Vorberg, 2015; Landman, Spekreijse, & Lamme, 2003; O'Herron & von der Heydt, 2011; Shioiri & Cavanagh, 1992; Supèr, Spekreijse, & Lamme, 2001; Wallis, Williams, & Arnold, 2009; Wutz, Weisz, Braun, & Melcher, 2014). The relatively long duration of contour persistence is remarkable in its own right, and may reflect the size of the underlying neural network (Compte, Brunel, Goldman-Rakic, & Wang, 2000; Toyoizumi, 2012).

The first published study of contour persistence focused on the maintenance of motion-defined groupings in object-selective lateral occipital cortex (Ferber et al., 2003), well beyond the cortical locus of an association-field in V1. Unlike V1 neurons, neurons in lateral occipital cortex (LOC) represent a shape independent of the physical properties of its defining contour (Altmann, Bülthoff, & Kourtzi, 2003; Kourtzi & Kanwisher, 2001). Thus, visual persistence of contour-defined form limited to LOC would suggest that V1 merely sends feedforward signals to LOC, in contrast to evidence that V1 and LOC are part of a recurrent contour-processing circuit (Drewes, Goren, Zhu, & Elder, 2016; Shpaner, Molholm, Forde, & Foxe, 2013; Wokke, Vandenbroucke, Scholte, & Lamme, 2013). A study by Strother et al. (2012) showed that persistent neural activity could be traced to the retinotopically defined representation of a contour in primary visual cortex, which supports the possibility that contour persistence is rooted in the sustained activation of low-level (e.g., V1) contour-integration mechanisms. In support of this possibility, previous studies have shown that scrambling contour elements and increasing interelement distance can decrease the duration of contour persistence (Ferber et al., 2005; Ferber & Emrich, 2007; Strother & Alferov, 2014), but none of these studies systematically manipulated interelement orientation, as in more traditional psychophysical studies of contour integration. In Experiment 1 we measured the effect of contour smoothness on visual persistence and distinguished this effect from observer bias. In Experiments 2 and 3 we studied the effects of contour smoothness and observer bias using different methods, which allowed us to further differentiate the respective contributions of these two distinct factors across different stimuli and tasks.

Methods

Subjects

Eighteen volunteers (20–36 years of age; six women; all were unaware of the purposes of the study except for one of the authors) participated in all three experiments. All observers were right-handed, with normal or corrected-to-normal vision. Informed consent was collected and the study was approved by the institutional review board of the University of Nevada, Reno.

Apparatus

All experiments were conducted using a 20-in. Dell Trinitron P991 monitor (1024 × 768 resolution) with an 85-Hz refresh rate. The stimulus computer was a 2.4-GHz Mac Mini with an Nvidia GeForce 320M graphics processor (256 MB of DDR2 SDRAM). Stimuli were created and presented using Psychtoolbox-3 (Kleiner et al., 2007) for MATLAB (MathWorks Inc., Natick, MA). Participants viewed stimuli binocularly from a distance of 60 cm in all three experiments.

Experiment 1: Contour persistence

Stimuli and procedure

In a dim room, participants viewed arrays of short black line segments (0.3° × 0.03°) against a white background upon which additional line segments forming a circular contour were superimposed after a brief delay (Figure 1). Observers were instructed to fixate a blue cross (0.3° × 0.3°) at the center of the screen and press a button when the contour circle was no longer visible. On each trial, the background array was presented first, and after 2 s a contour circle appeared with abrupt onset against the background array, always centered within the aperture (https://sites.google.com/site/experimentdemos/). Background line-segment arrays consisted of 3,250 line segments displayed across the

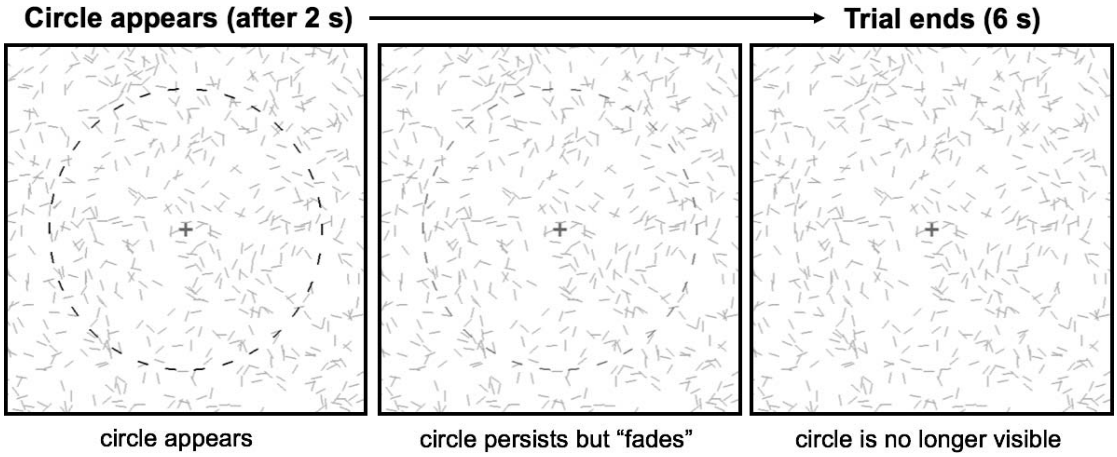

Figure 1. Illustration of contour persistence during a trial. Once a contour circle appeared against a camouflaging background, it was perceived to fade even though its constituent elements remained superimposed on the background. The task of observers was to indicate when the circle was no longer visible. Although the colors of line segments belonging to circle and background differ here for purpose of illustration, all line segments were black in the experiment.

entire screen (36.9° × 28.1°), with a density of approximately 3.13 segments/$^{\circ 2}$. Circle contour segments covered 40% of the of the contour circle's circumference. Both the background and the embedded circle remained on the screen for 6 s, during which time observers responded with a button press indicating when they could no longer see the circle. It is important to note that although the circle and background did not change physically during this time, circles appeared to fade into the background. After the 6-s response period, the screen went blank for 1 s and the next trial began. This cycle repeated until the end of the experiment.

The radii of contour circles were either 1.5°, 3°, or 4.5° to create uncertainty with respect to contour location in visual field. The smoothness of the circular contour was manipulated by changing the range of the angle α between line segments and corresponding tangents to the circular path (Figure 2a), which varied from 0° (smooth and cocircular) to 60° (jagged circles composed of line segments with randomly varying α between 0° and 60°). Contour smoothness was restricted between 0° and 60° (in 10° increments) because results of a pilot study indicated no change in visibility between 60° and 90°; Figure 2b shows examples. Contour-circle radii were changed trial by trial in order to reduce predictability and avoid potential adaptation effects. All combinations of jitter and circle size were implemented randomly within the cycle of experimental trials. Observers completed 20 practice trials, then 20 to 30 trials for each of the seven levels of contour smoothness (for a minimum total of 140 and a maximum total of 210 experiment trials over the course of approximately 35 min, with three opportunities to rest).

Results and discussion

We measured and analyzed the duration of visual persistence based on observers' response times (RTs), which indicated when a previously visible contour had disappeared. Circle size was allowed to vary randomly to increase observer uncertainty with respect to contour location (eccentricity), but we do not include this variable in any of the analyses reported here, due to the limited number of trials per condition per observer (for effects of circle size, see Strother & Alferov, 2014).

The leftmost graph in Figure 3 is a scatter plot of individual observers' mean RTs at each level of α, fitted

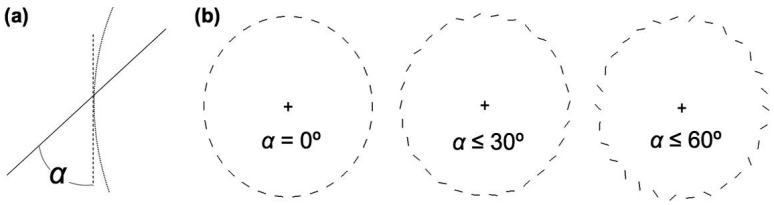

Figure 2. The smoothness of contour circles was allowed to vary as a function of α, the angle between a contour element and a tangent to the circle, as shown in (a). Three examples are shown in (b); as α increases, circle contours become less smooth. Note that α is not fixed, and the value of α is the maximum deviation of the orientation of a contour element from the tangent to the circle at the location of the element.

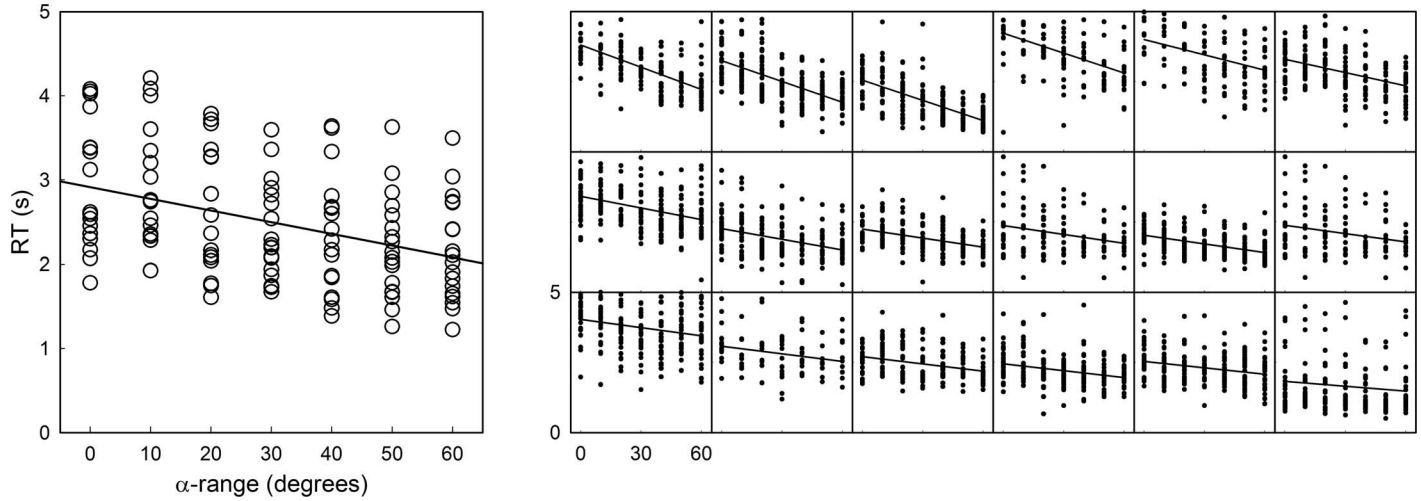

Figure 3. Results from Experiment 1. The leftmost graph is a scatter plot of individual observers' mean response times, indicating duration of contour persistence at each level of α. The negative slope of the regression line indicates decreasing persistence with decreases in contour smoothness. The right graphs show scatter plots and regression lines for individual observers (plotted on the same scale as the group results), sorted by decreasing smoothness sensitivity.

with a regression line. Mean RT averaged across all α levels was 2.50 s. RTs were longest for $\alpha = 0°$ ($M = 2.92$ s) and shortest for $\alpha = 60°$ ($M = 2.16$ s), indicating an overall difference of 0.76 s between the two most extreme contour-smoothness conditions. A group-level linear-regression analysis of the effect of α on RT was highly significant, $R^2 = 0.15$, $F(1, 124) = 22.04$, $p < 0.001$, with a slope of $B = -0.014$ s/°, which means that the duration of persistence decreased as the contour became less aligned. We computed a slope-to-intercept ratio by dividing 0.76 (computed earlier in this paragraph) by the intercept ($B_0 = 2.92$) of the linear model. The value of this ratio (SI), which could vary from 0 to 1, was SI = 0.26. SI quantifies the contribution of an effect of α to the overall range of RTs at the group level.

In addition to our group-level analysis, we performed linear-regression analyses on individual observers' data in order to obtain operationally defined measures of individuals' *sensitivity* to α (regression coefficients) and also individual observer *bias*, measured as mean RT (averaged across all α levels). The matrix of graphs in Figure 3 shows data and regression lines for individual observers. In agreement with our group-level analyses, linear-regression analyses for all except one observer (whose slope was nevertheless negative) were statistically significant (all ps < 0.05; mean $R^2 = 0.15$ when calculated from R^2 for individual observers). The range of α sensitivities was −0.026 to −0.006 s/° ($M = -0.014$ s/°, $SD = 0.007$ s/°), and the range of bias was 1.65 to 3.75 s ($M = 2.50$ s, $SD = 0.64$ s). As we did earlier at the group level, we computed the SI for each individual, which ranged from 0.13 to 0.51 ($M = 0.26$, identical for that computed at the group level). This result means that smoothness sensitivity accounted for different degrees of persistence across individuals; we return to SI in between-experiments analyses reported later.

Finally, we performed a Pearson correlation on sensitivity and bias and found that the two measures were not correlated, $r(16) = -0.35$, $p = 0.15$. On one hand this could be interpreted to suggest that α sensitivity and bias to report contour disappearance are independent, if the joint distribution of individuals' sensitivity and bias measures is Gaussian (which we confirmed for our current data using multiple convergent statistical approaches, including a multivariate Shapiro–Wilk test to test the null hypothesis that the sample data are from a multivariate normal distribution). On the other hand, our sample size of 18 subjects severely limits our confidence in this interpretation. To reach a level of statistical power ($1 - \beta$) of 0.8, we would have to increase our sample size to more than 60 subjects (G*Power; Faul, Erdfelder, Lang, & Buchner, 2007).

Experiment 2: Background *accretion* and contour hysteresis

Stimuli and procedure

In this experiment we used a novel paradigm to investigate the hysteresis of contour visibility as a function of contour smoothness in the context of *increasing* background density. On each trial, a contour circle was presented in the absence of a background, and 30 ms after its onset, background line segments were added at a rate of 15 line segments per 30 ms

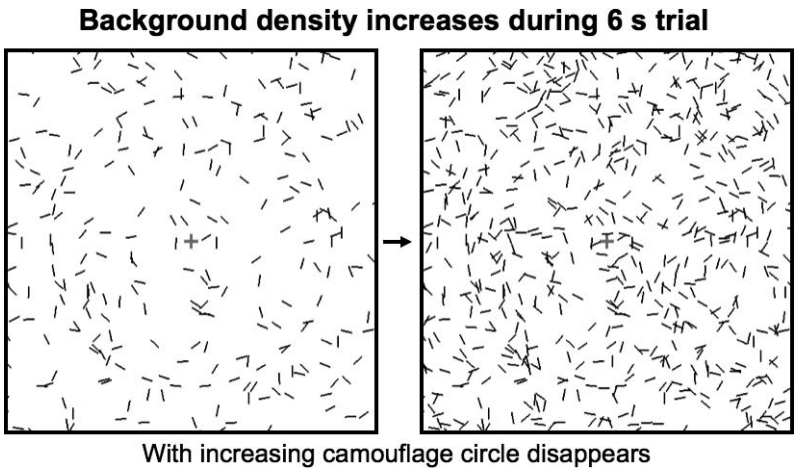

Figure 4. Illustration of trial in which a circular contour becomes increasingly camouflaged as the density of the background is increased. Background changes were always incremental, and observers indicated when they could no longer see the circle.

(Figure 4); this processes looped and 15 background line segments were added simultaneously during each iteration (https://sites.google.com/site/experimentdemos/). Observers were instructed to press a button as soon the contour circle became fully camouflaged by the accreting background (number of background elements present at time of button press was the dependent measure). Properties of the contour circle (radii, line-segment size, orientations, and spacing within the circular contour) were identical to those of the contour circles used in Experiment 1, as were the fixation instructions, number of trials, 1-s intertrial interval, and opportunities for breaks.

Results and discussion

To measure the effect of contour smoothness on hysteresis (continued visibility under conditions of increasing background density), we recorded the density of dynamic, increasingly camouflaged background at the point when observers indicated that a previously visible contour had disappeared, and we used this density measure as the dependent variable for our statistical analyses.

The leftmost graph in Figure 5 is a scatter plot of individual observers' data at each level of α fit with a regression line. Mean density averaged across all α levels was 1.98 segments/$^{\circ 2}$. Densities were greatest for $\alpha = 0^{\circ}$ ($M = 2.47$ segments/$^{\circ 2}$) and lowest for $\alpha = 60^{\circ}$ ($M = 1.55$ segments/$^{\circ 2}$), indicating an overall difference of 0.92 segments/$^{\circ 2}$ between the two most extreme contour-smoothness conditions. A group linear-regression analysis of the effect of α on hysteresis was highly significant, $B = -0.017$ segments/$^{\circ 2}$ per jitter degree, $R^2 = 0.27$, $F(1, 124) = 45.91$, $p < 0.001$, which means that contour visibility was retained at greater background densities for lower levels of α (greater smoothness). We computed SI by dividing 0.92 (computed earlier) by the intercept ($B_0 = 2.48$) of the linear model, for SI = 0.37. The SI for this experiment was greater than that for Experiment 1 (SI = 0.26).

As in Experiment 1, we performed linear-regression analyses on individual observers' data in order to obtain measures of sensitivity and bias. The matrix of graphs in Figure 5 shows regression lines for individual observers. Linear-regression analyses were statistically significant for all observers (all ps < 0.05; mean $R^2 = 0.35$ when calculated from R^2 for individual observers). The range of regression coefficients (sensitivities) was -0.030 to -0.005 segments/$^{\circ 2}$ per jitter degree ($M = -0.017$ segments/$^{\circ 2}$ per jitter degree, $SD = 0.007$ segments/$^{\circ 2}$ per jitter degree), and the range of background densities averaged across α (bias) was 0.80 to 2.73 segments/$^{\circ 2}$ ($M = 1.98$, $SD = 0.54$). As we did earlier at the group level, we computed an SI for each individual, which ranged from 0.17 to 0.53 ($M = 0.37$, identical to that computed at the group level), which means that smoothness sensitivity accounted for different degrees of hysteresis across individuals. Pearson correlation showed that the slope and mean were correlated such that steeper slopes were correlated with greater degrees of bias, $r(16) = -0.60$, $p < 0.01$. We return to this and comparisons of SI across experiments in a later section.

Experiment 3: Background *deletion* and contour detection

Stimuli and procedure

In this experiment we investigated the detectability of contours embedded within a background of *decreasing* density as a function of contour smoothness.

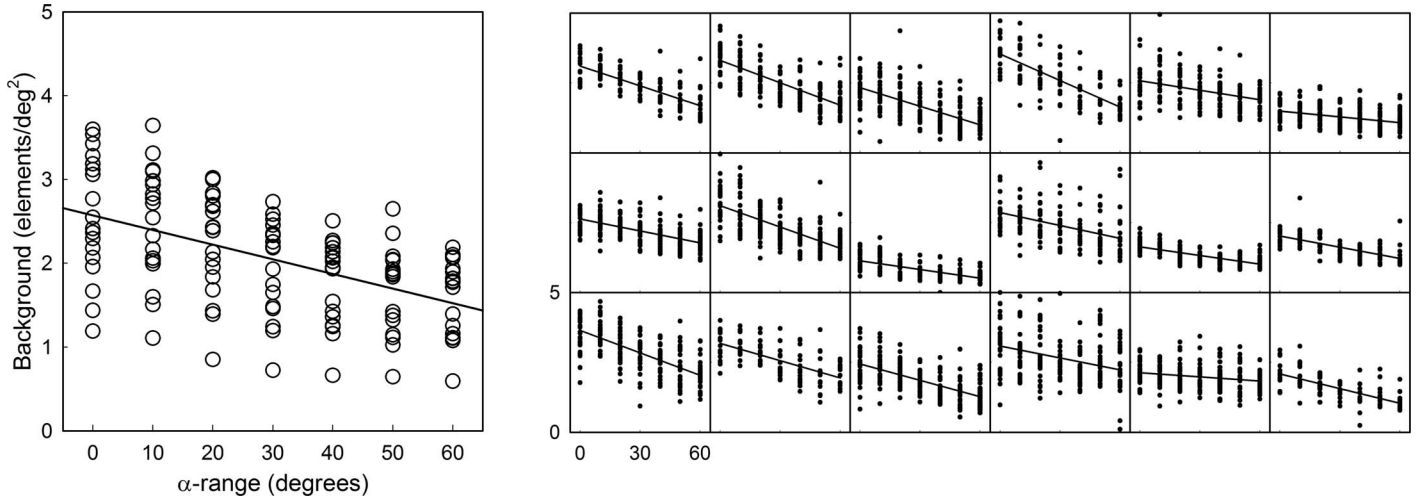

Figure 5. Results from Experiment 2. The leftmost graph is a scatter plot of background densities, for each level of α, at which observers reported the contour circle to disappear. The negative slope of the regression line means that with decreases in contour smoothness, a progressively less dense background was required for full camouflage. The right graphs show scatter plots and regression lines for individual observers (plotted on the same scale as the group results) in the same order as in Figure 3.

On each trial, a contour circle fully camouflaged by a dense array of background line segments gradually became visible as background line segments were removed (Figure 6). As in Experiment 2, the process of changing the background began 30 ms into the trial, after which the 5,000 background line segments were gradually reduced to zero by the end of the trial (https://sites.google.com/site/experimentdemos/). Line segments were removed at a rate of 15 line segments per 30 ms for the first 3,000 line segments and 10 line segments per loop iteration for the remaining 2,000 line segments. Pilot results showed that high line-segment deletion rates late in the trial resulted in an inability of observers to respond prior to the complete disappearance of the background (as in Experiment 2, the dependent measure was the number of background elements at the time of button press).

Results and discussion

To measure the effect of contour smoothness on contour detection, we recorded the density of dynamic, increasingly camouflaged background at the point when observers indicated that a completely camouflaged contour became visible, and we used this as the dependent variable for our analyses.

The leftmost graph in Figure 7 is a scatter plot of individual observers' data at each level of α fitted with a regression line. Mean density averaged across all α levels was 1.18 segments/$^{\circ 2}$ (as compared to 1.98

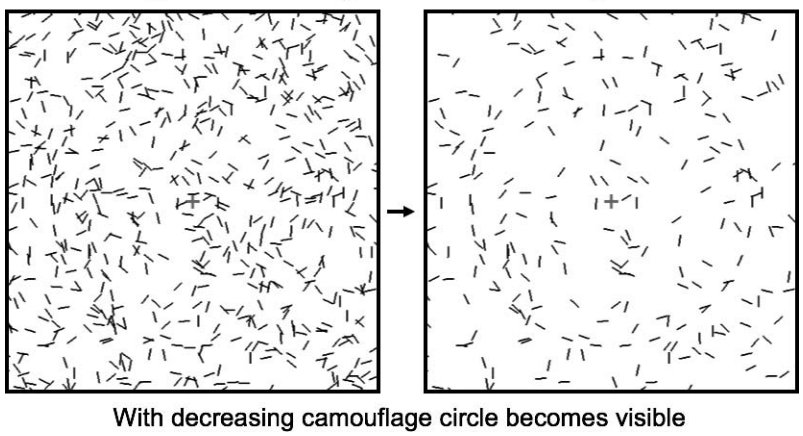

Figure 6. Illustration of trial in which a circular contour becomes increasingly visible as the density of the background is decreased. Background changes were always incremental, and observers indicated when a camouflaged circle became visible.

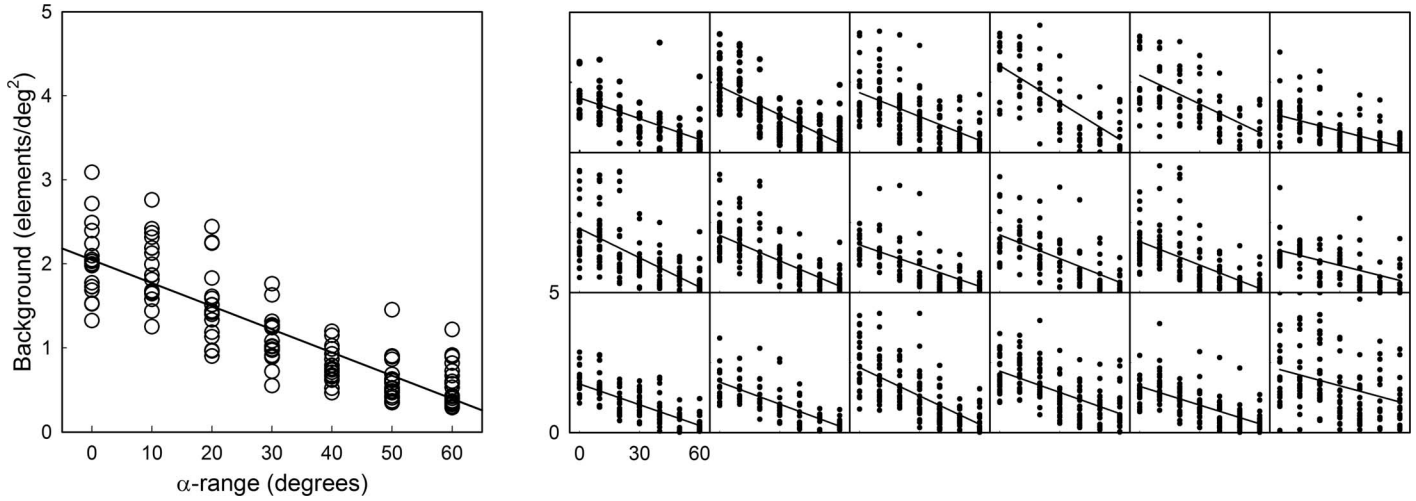

Figure 7. Results from Experiment 3. The leftmost graph is a scatter plot of background densities (plotted on same scale as Experiment 2; see Figure 5), for each level of α, at which observers reported that a contour circle became visible. The negative slope of the regression line means that with decreases in contour smoothness, a progressively less dense background was required for contour visibility. The right graphs show scatter plots and regression lines for individual observers (plotted on the same scale as the group results) in the same order as in Figures 3 and 5.

segments/°^{2} in Experiment 2). Densities were greatest for $\alpha = 0°$ ($M = 1.95$ segments/°^{2}) and lowest for $\alpha = 60°$ ($M = 0.55$ segments/°^{2}), indicating an overall difference of 1.40 segments/°^{2} (as compared to 0.92 segments/°^{2} in Experiment 2) between the two most extreme contour-smoothness conditions. As expected, a group linear-regression analysis of the effect of α on detectability was highly significant, $B = -0.027$ segments/deg^2 per jitter degree, $R^2 = 0.71$, $F(1, 124) = 304.29$, $p < 0.001$, which means that the necessary density of the background to maintain full camouflage decreased as the contour became less smooth. We computed SI by dividing 1.40 (computed earlier) by the intercept ($B_0 = 1.97$) of the linear model, for SI = 0.71. The SI for this experiment was greater than those for Experiments 1 and 2 (0.26 and 0.37, respectively).

As in the previous experiments, we performed linear-regression analyses on individual observers' data in order to obtain measures of sensitivity and bias. The matrix of graphs in Figure 7 shows regression lines for individual observers. Linear-regression analyses were statistically significant for all observers (all ps < 0.05; mean $R^2 = 0.39$ when calculated from R^2 for individual observers). The range of regression coefficients was −0.042 to −0.017 segments/°^{2} per jitter degree (M = −0.027 segments/°^{2} per jitter degree, $SD = 0.006$ segments/°^{2} per jitter degree), and the range of means was 0.76 to 1.82 segments/°^{2} ($M = 1.21$ segments/°^{2}, $SD = 0.29$ segments/°^{2}). We again computed an SI for each individual, which ranged from 0.36 to 0.81 ($M = 0.71$, identical for that computed at the group level); this means that smoothness sensitivity accounted for different degrees of detectability across individuals, and the higher mean (0.71, as compared to 0.37 for Experiment 2) indicates a relatively stronger effect of α in this experiment. Pearson correlation showed that the slope and mean were correlated, $r(16) = -0.61$, $p < 0.01$.

Post hoc between-experiments analyses

In addition to conducting correlation analyses on the sensitivity and bias measures within each experiment, we assessed potential correlations between these measures between the three experiments. We found that sensitivity to changes in α was positively correlated across all three experiments: Pearson correlation of sensitivity in Experiment 1 (contour persistence) and Experiment 2 (contour hysteresis) was $r(16) = 0.48$, $p = 0.043$; in Experiment 1 (contour persistence) and Experiment 3 (contour detection), $r(16) = 0.47$, $p = 0.048$; and in Experiment 2 (contour hysteresis) and Experiment 3 (contour detection), $r(16) = 0.52$, $p = 0.026$. We also performed correlation analyses on individual observer bias: Pearson correlation of sensitivity in Experiment 1 (contour persistence) and Experiment 2 (contour hysteresis) was $r(16) = 0.56$, $p = 0.015$; in Experiment 1 (contour persistence) and Experiment 3 (contour detection), $r(16) = 0.22$, $p = 0.39$; and in Experiment 2 (contour hysteresis) and Experiment 3 (contour detection), $r(16) = 0.34$, $p = 0.17$. It should be noted that because our power is severely limited due to our sample size (see Experiment 1, Results and discussion), we must exercise caution when

interpreting the statistical significance of these correlations. However, our observation of exclusively positive correlation coefficients could mean that any reliably significant correlations are more likely to be positive than negative.

Given the limitations of our correlation analyses, which sought to assess predictability of individuals' smoothness sensitivity and bias between experiments, we performed additional analyses to examine changes in sensitivity and bias across experiments. We compared the results of the linear regressions performed for each experiment, as well as the means and SIs (reported in Results and discussion for each experiment), and conducted additional analyses on normalized results (to allow for direct comparisons of sensitivity and bias between experiments).

A one-way repeated-measures ANOVA on the previously reported R^2 values for individuals, across experiments, revealed a significant main effect of experiment, $F(2, 34) = 22.71$, $p < 0.001$. Paired comparison showed that R^2 for Experiment 1 was smaller than for Experiments 2 and 3, but that there was no difference in R^2 values between Experiments 2 and 3. The relatively low R^2 value for Experiment 1 can be explained in part by the relatively higher overall variability of observer bias (means). One-way repeated-measures ANOVAs on the slopes (sensitivity) and means (bias) for normalized data were supportive of this explanation—for slopes, $F(2, 34) = 66.75$, $p < 0.001$; for means, $F(2, 34) = 17.56$, $p < 0.001$. The means were greater and more variable in Experiment 1 ($M = 0.39$, $SD = 0.11$) than in Experiment 2 ($M = 0.33$, $SD = 0.09$) and Experiment 3 ($M = 0.25$, $SD = 0.06$); the slopes did not differ between Experiment 1 ($M = -0.0024$, $SD = 0.0012$) and Experiment 2 ($M = -0.0028$, $SD = 0.0012$), and the steepest slope was observed for Experiment 3 ($M = -0.0056$, with comparable variability, $SD = 0.0013$). In sum, our analyses of R^2 indicate that Experiment 1 showed the lowest R^2 due to the relatively high degree of variability (SD) in observer bias as compared to the other two experiments. Taken together with the previously reported SIs for each experiment (with SI increasing from Experiment 1 to Experiment 2 to Experiment 3), our results suggest that the relative contributions of smoothness sensitivity and observer bias were different across experiments. Specifically, bias exerted the strongest and most variable effect in Experiment 1, and weakest and least variable effect in Experiment 3. In short, our ANOVA results—which did not suffer from the limited statistical power of our correlation analyses—highlight differences in sensitivities and bias across experiments, with bias playing the greatest role in Experiment 1 and sensitivity playing the greatest role in Experiment 3.

General discussion

We performed three experiments to examine the effect of contour smoothness on contour visibility under conditions of impending camouflage. We were especially interested in distinguishing the expected effects of contour smoothness on contour persistence from response bias, both of which were highly variable across individual observers. In all three experiments we observed an effect of contour smoothness, in both group-level and individual-level analyses, such that camouflaged contours became less visible against a highly camouflaging background as contour smoothness was decreased. In Experiment 1 this was evident in increasing persistence with increasing contour smoothness. In Experiment 2, increasing contour smoothness resulted in enhanced visibility against an increasingly dense background, and in Experiment 3 increasing smoothness resulted in increased detectability against a decreasingly dense background. We observed an additional effect of bias, which we differentiated from the effect of contour smoothness in terms of both its variability across observers and experiments and its contribution relative to smoothness sensitivity. Bias was strongest and most variable in Experiment 1 (contour persistence), which may be related to a greater degree of uncertainty about a contour disappearing in a physically unchanging stimulus (in Experiment 2, contours disappeared in the context of a dynamic, increasingly dense background) or a becoming visible as opposed to disappearing (Experiment 3).

The observed effects of contour smoothness are consistent with the involvement of an association-field (AF) mechanism of contour integration (for reviews, see Hess & Field, 1999; Hess, Hayes, & Field, 2003) in contour perception under different types of camouflaging conditions. However, our observation of facilitative effects of increasing contour smoothness was not a foregone conclusion, especially given contrary findings from other studies that used highly camouflaged circular contours. For example, a study by Schmidtmann, Gordon, Bennett, and Loffler (2013) showed that the detectability of circular contours composed of oriented wavelets was not influenced by the relative orientation of the wavelets (and was also not dependent upon the deviation of wavelet position from a circular path). The authors concluded that the detection of such stimuli under conditions of camouflage need not engage mechanisms sensitive to contour smoothness, such as the AF. On the other hand, a study of the prospective effect of closure on contour integration by Tversky, Geisler, and Perry (2004)—which also used circular contour stimuli—reported results consistent with ours, such that decreasing smoothness of a contour, whether closed or not,

predicted its visibility. In sum, there is evidence of a primary role of global form in the detection of a camouflaged circular contour field (for relevant reviews, see Loffler, 2008, 2015), as well as evidence that contour smoothness is important, including the results reported here and in an earlier study (Strother & Alferov, 2014).

While the effects of contour smoothness in all of our experiments are consistent with the operation of an AF or similar mechanism, our results do not necessarily preclude the involvement of a purely global visual mechanism. Indeed, with respect to contour persistence (Experiment 1), a previous result by Strother et al. (2011) showed that inversion of a contour-defined shape (the outline of a face or animal) reduced its persistence even though contour smoothness was unchanged. Those researchers proposed that the visual persistence of global form is influenced by stimulus familiarity and shape-related feedback to early visual areas, including V1. The results reported here complement the effects of familiarity and global shape on visual persistence reported in that study, as well as related effects on contour detection (Sassi, Demeyer, Machilsen, Putzeys, & Wagemans, 2014). One possibility is that feedback from shape-selective visual areas (e.g., V4 and higher tier visual areas) interacts with a smoothness-sensitive (e.g., AF) mechanism in V1, and that all else being equal (i.e., global shape always being a circle), contour smoothness concomitantly modulates the operation of both V1 and higher tier shape-processing mechanisms.

As discussed earlier, the effects of contour smoothness varied quantitatively across individuals and across experiments, but nevertheless always showed the same qualitative effect—although the coefficients varied from subject to subject, the corresponding slopes were always negative, indicating a facilitative effect of increasing contour smoothness on persistence, and visibility in general. Comparisons of the degree of interindividual variability in smoothness sensitivity across experiments (using standard deviations of normalized data) showed considerable similarity, although the magnitude of slopes tended to be greater in Experiment 3 than in the other two experiments. This means that even when the magnitude of the slope varied, the range of slopes was stable across experiments, which indicates consistency of smoothness sensitivity across tasks, in contrast to the predictions of other studies that show dependence of early visual processing on task and context (Gilbert & Li, 2013; Qiu, Burton, Kersten, & Olman, 2016; Robol, Casco, & Dakin, 2012). Furthermore, the results of our correlation analyses (though statistically underpowered) in combination with additional between-experiments analyses (e.g., of R^2 and SI) suggest that even though the relative contributions of sensitivity and bias are distinct across experiments, sensitivity was relatively stable.

Our finding of relatively stable smoothness sensitivity with respect to bias is consistent with the possibility of independent mechanisms—for example, the AF mechanism for smoothness sensitivity and a bias mechanism that exists within the visual system or beyond. If intrinsic reverberation of the AF mechanism is the low-level basis of contour persistence, top-down feedback—which plays an important role in contour integration more generally (Gilbert & Li, 2013)—may modulate the duration of its reverberation without altering its sensitivity. Alternatively, one could argue that a smoothness-sensitive contour-integration mechanism (e.g., in V1) merely passes on a stronger input to a higher tier shape representation (e.g., in LOC; Altmann et al., 2003; Fang, Kersten, & Murray, 2008; Kourtzi, Tolias, Altmann, Augath, & Logothetis, 2003) which serves as the locus of persistence, as proposed in the first study of contour persistence (Ferber et al., 2003). If so, then the longer duration of persistence for smooth contours would be due to the effect of contour smoothness on the initial input to this representation, with stronger input for smoother contours. However, if this were the case, then early visual cortex (e.g., V1) would not need to participate after relaying its inputs to higher tier areas like LOC. Two fMRI studies by Strother and colleagues showed that this is not the case, and that contour-specific neural activity in V1 was correlated with the duration of contour persistence (Strother et al., 2011; Strother et al., 2012). Their findings were consistent with the idea that rather than passively inheriting input from early visual cortex, a V1–LOC positive-feedback loop performs recurrent input verification (i.e., checking whether or not contour edges have been physically removed) to sustain a persistent contour representation. This behavior of the V1–LOC circuit during contour persistence is consistent with recent neurophysiological findings (Drewes et al., 2016) and may be related to "input filtering" in the context of masking and visible persistence (Patten et al., 2015).

In conclusion, although contour persistence appears to reflect a confluence of smoothness sensitivity and bias, the respective contribution of each is distinct. We previously speculated about the involvement of an AF mechanism in contour persistence (Strother et al., 2012; Strother & Alferov, 2014), in addition to top-down effects related to the recognition of a contour-defined object (Emrich, Ruppel, & Ferber, 2008; Strother et al., 2011). However, this study is the first to test this possibility systematically. Our results may be relevant to models of persistent contour processing in the absence of positive feedback-loop resetting (e.g., Francis et al., 1994; Grossberg, 2015). We propose that, while global shape-processing mechanisms may also

play an important role in contour persistence, the AF or other similar mechanism of contour integration provides a fundamental neural basis of object continuity in both space and time.

Keywords: visual persistence, contour integration, camouflage, hysteresis, memory, reverberation, visual cortex

Acknowledgments

Research reported in this publication was supported by the National Institute of General Medical Sciences (P20 GM103650).

Commercial relationships: none.
Corresponding author: Lars Strother.
Email: lars@unr.edu.
Address: Department of Psychology, University of Nevada, Reno, NV, USA.

References

Altmann, C. F., Bülthoff, H. H., & Kourtzi, Z. (2003). Perceptual organization of local elements into global shapes in the human visual cortex. *Current Biology*, *13*(4), 342–349.

Bruchmann, M., Thaler, K., & Vorberg, D. (2015). Visible persistence of single-transient random dot patterns: Spatial parameters affect the duration of fading percepts. *PLoS One*, *10*(9), e0137091, doi:10.1371/journal.pone.0137091.

Compte, A., Brunel, N., Goldman-Rakic, P. S., & Wang, X. J. (2000). Synaptic mechanisms and network dynamics underlying spatial working memory in a cortical network model. *Cerebral Cortex*, *10*(9), 910–923.

Drewes, J., Goren, G., Zhu, W., & Elder, J. H. (2016). Recurrent processing in the formation of shape percepts. *The Journal of Neuroscience*, *36*(1), 185–192, doi:10.1523/JNEUROSCI.2347-15.2016.

Emrich, S. M., Ruppel, J. D., & Ferber, S. (2008). The role of elaboration in the persistence of awareness for degraded objects. *Consciousness and Cognition*, *17*(1), 319–329, doi:10.1016/j.concog.2006.12.001.

Fang, F., Kersten, D., & Murray, S. O. (2008). Perceptual grouping and inverse fMRI activity patterns in human visual cortex. *Journal of Vision*, *8*(7):2, 1–9, doi:10.1167/8.7.2. [PubMed] [Article]

Faul, F., Erdfelder, E., Lang, A. G., & Buchner, A. (2007). G*Power 3: A flexible statistical power analysis program for the social, behavioral, and biomedical sciences. *Behavioral Research Methods*, *39*(2), 175–191.

Ferber, S., & Emrich, S. M. (2007). Maintaining the ties that bind: The role of an intermediate visual memory store in the persistence of awareness. *Cognitive Neuropsychology*, *24*(2), 187–210, doi:10.1080/02643290601046598.

Ferber, S., Humphrey, G. K., & Vilis, T. (2003). The lateral occipital complex subserves the perceptual persistence of motion-defined groupings. *Cerebral Cortex*, *13*(7), 716–721.

Ferber, S., Humphrey, G. K., & Vilis, T. (2005). Segregation and persistence of form in the lateral occipital complex. *Neuropsychologia*, *43*(1), 41–51, doi:10.1016/j.neuropsychologia.2004.06.020.

Field, D. J., Hayes, A., & Hess, R. F. (1993). Contour integration by the human visual system: Evidence for a local "association field." *Vision Research*, *33*(2), 173–193, doi:10.1016/0042-6989(93)90156-Q.

Francis, G. (1996). Cortical dynamics of lateral inhibition: Visual persistence and ISI. *Attention, Perception, & Psychophysics*, *58*(7), 1103–1109.

Francis, G. (1999). Spatial frequency and visual persistence: Cortical reset. *Spatial Vision*, *12*(1), 31–50.

Francis, G., Grossberg, S., & Mingolla, E. (1994). Cortical dynamics of feature binding and reset: Control of visual persistence. *Vision Research*, *34*(8), 1089–1104.

Geisler, W. S., & Perry, J. S. (2009). Contour statistics in natural images: Grouping across occlusions. *Visual Neuroscience*, *26*(1), 109–121, doi:10.1017/S0952523808080875.

Geisler, W. S., Perry, J. S., Super, B. J., & Gallogly, D. P. (2001). Edge co-occurrence in natural images predicts contour grouping performance. *Vision Research*, *41*(6), 711–724.

Gilbert, C. D., & Li, W. (2013). Top-down influences on visual processing. *Nature Reviews Neuroscience*, *14*(5), 350–363, doi:10.1038/nrn3476.

Grossberg, S. (2015). Cortical dynamics of figure-ground separation in response to 2D pictures and 3D scenes: How V2 combines border ownership, stereoscopic cues, and gestalt grouping rules. *Frontiers in Psychology*, *6*, 2054, doi:10.3389/fpsyg.2015.02054.

Hess, R., & Field, D. (1999). Integration of contours: New insights. *Trends in Cognitive Science*, *3*(12), 480–486.

Hess, R. F., Hayes, A., & Field, D. J. (2003). Contour integration and cortical processing. *Journal of*

Physiology–Paris, *97*(2–3), 105–119, doi:10.1016/j.jphysparis.2003.09.013.

Kleiner, M., Brainard, D., Pelli, D., Ingling, A., Murray, R., & Broussard, C. (2007). What's new in Psychtoolbox-3. *Perception*, *36*(14), 1.

Kourtzi, Z., & Kanwisher, N. (2001, Aug 24). Representation of perceived object shape by the human lateral occipital complex. *Science*, *293*(5534), 1506–1509, doi:10.1126/science.1061133.

Kourtzi, Z., Tolias, A. S., Altmann, C. F., Augath, M., & Logothetis, N. K. (2003). Integration of local features into global shapes: Monkey and human FMRI studies. *Neuron*, *37*(2), 333–346.

Landman, R., Spekreijse, H., & Lamme, V. A. (2003). Large capacity storage of integrated objects before change blindness. *Vision Research*, *43*(2), 149–164.

Large, M. E., Aldcroft, A., & Vilis, T. (2005). Perceptual continuity and the emergence of perceptual persistence in the ventral visual pathway. *Journal of Neurophysiology*, *93*(6), 3453–3462.

Li, Z. (1998). A neural model of contour integration in the primary visual cortex. *Neural Computation*, *10*(4), 903–940.

Loffler, G. (2008). Perception of contours and shapes: Low and intermediate stage mechanisms. *Vision Research*, *48*(20), 2106–2127, doi:10.1016/j.visres.2008.03.006.

Loffler, G. (2015). Probing intermediate stages of shape processing. *Journal of Vision*, *15*(7):1, 1–19, doi:10.1167/15.7.1. [PubMed] [Article]

O'Herron, P., & von der Heydt, R. (2009). Short-term memory for figure-ground organization in the visual cortex. *Neuron*, *61*(5), 801–809, doi:10.1016/j.neuron.2009.01.014.

O'Herron, P., & von der Heydt, R. (2011). Representation of object continuity in the visual cortex. *Journal of Vision*, *11*(2):12, 1–9, doi:10.1167/11.2.12. [PubMed] [Article]

Patten, J. W., Lagroix, H. E., Dixon, P., Di Lollo, V., Sager, B., Jannati, A., ... Spalek, T. M. (2015). Escape from temporal-integration masking: The roles of visible persistence and input filtering. *Journal of Experimental Psychology: Human Perception and Performance*, *41*(2), 431–440, doi:10.1037/a0038903.

Qiu, C., Burton, P. C., Kersten, D., & Olman, C. A. (2016). Responses in early visual areas to contour integration are context dependent. *Journal of Vision*, *16*(8):19, 1–18, doi:10.1167/16.8.19. [PubMed] [Article]

Regan, D. (1986). Form from motion parallax and form from luminance contrast: Vernier discrimination. *Spatial Vision*, *1*(4), 305–318.

Robol, V., Casco, C., & Dakin, S. C. (2012). The role of crowding in contextual influences on contour integration. *Journal of Vision*, *12*(7):3, 1–18, doi:10.1167/12.7.3. [PubMed] [Article]

Sassi, M., Demeyer, M., Machilsen, B., Putzeys, T., & Wagemans, J. (2014). Both predictability and familiarity facilitate contour integration. *Journal of Vision*, *14*(5):11, 1–15, doi:10.1167/14.5.11. [PubMed] [Article]

Schmidtmann, G., Gordon, G. E., Bennett, D. M., & Loffler, G. (2013). Detecting shapes in noise: Tuning characteristics of global shape mechanisms. *Frontiers in Computational Neuroscience*, *7*, 37, doi:10.3389/fncom.2013.00037.

Shioiri, S., & Cavanagh, P. (1992). Visual persistence of figures defined by relative motion. *Vision Research*, *32*(5), 943–951.

Shpaner, M., Molholm, S., Forde, E., & Foxe, J. J. (2013). Disambiguating the roles of area V1 and the lateral occipital complex (LOC) in contour integration. *NeuroImage*, *69*, 146–156, doi:10.1016/j.neuroimage.2012.11.023.

Sigman, M., Cecchi, G. A., Gilbert, C. D., & Magnasco, M. O. (2001). On a common circle: Natural scenes and Gestalt rules. *Proceedings of the National Academy of Sciences, USA*, *98*(4), 1935–1940, doi:10.1073/pnas.031571498.

Strother, L., & Alferov, D. (2014). Inter-element orientation and distance influence the duration of persistent contour integration. *Frontiers in Psychology*, *5*, 1273, doi:10.3389/fpsyg.2014.01273.

Strother, L., Lavell, C., & Vilis, T. (2012). Figure-ground representation and its decay in primary visual cortex. *Journal of Cognitive Neuroscience*, *24*(4), 905–914, doi:10.1162/jocn_a_00190.

Strother, L., Mathuranath, P. S., Aldcroft, A., Lavell, C., Goodale, M. A., & Vilis, T. (2011). Face inversion reduces the persistence of global form and its neural correlates. *PLoS One*, *6*(4), e18705, doi:10.1371/journal.pone.0018705.

Supèr, H., Spekreijse, H., & Lamme, V. A. (2001, Jul 6). A neural correlate of working memory in the monkey primary visual cortex. *Science*, *293*(5527), 120–124, doi:10.1126/science.1060496.

Toyoizumi, T. (2012). Nearly extensive sequential memory lifetime achieved by coupled nonlinear neurons. *Neural Computation*, *24*(10), 2678–2699, doi:10.1162/NECO_a_00324.

Tversky, T., Geisler, W. S., & Perry, J. S. (2004). Contour grouping: Closure effects are explained by

good continuation and proximity. *Vision Research*, *44*(24), 2769–2777, doi:10.1016/j.visres.2004.06.011.

Wallis, T. S., Williams, M. A., & Arnold, D. H. (2009). Pre-exposure to moving form enhances static form sensitivity. *PLoS One*, *4*(12), e8324, doi:10.1371/journal.pone.0008324.

Wokke, M. E., Vandenbroucke, A. R., Scholte, H. S., & Lamme, V. A. (2013). Confuse your illusion: Feedback to early visual cortex contributes to perceptual completion. *Psychological Science*, *24*(1), 63–71, doi:10.1177/0956797612449175.

Wutz, A., Weisz, N., Braun, C., & Melcher, D. (2014). Temporal windows in visual processing: "Prestimulus brain state" and "poststimulus phase reset" segregate visual transients on different temporal scales. *The Journal of Neuroscience*, *34*(4), 1554–1565, doi:10.1523/JNEUROSCI.3187-13.2014.